Article

Cell Stem Cell

Polycomb Complex PRC1 Preserves Intestinal Stem Cell Identity by Sustaining Wnt/β-Catenin Transcriptional Activity

Graphical Abstract

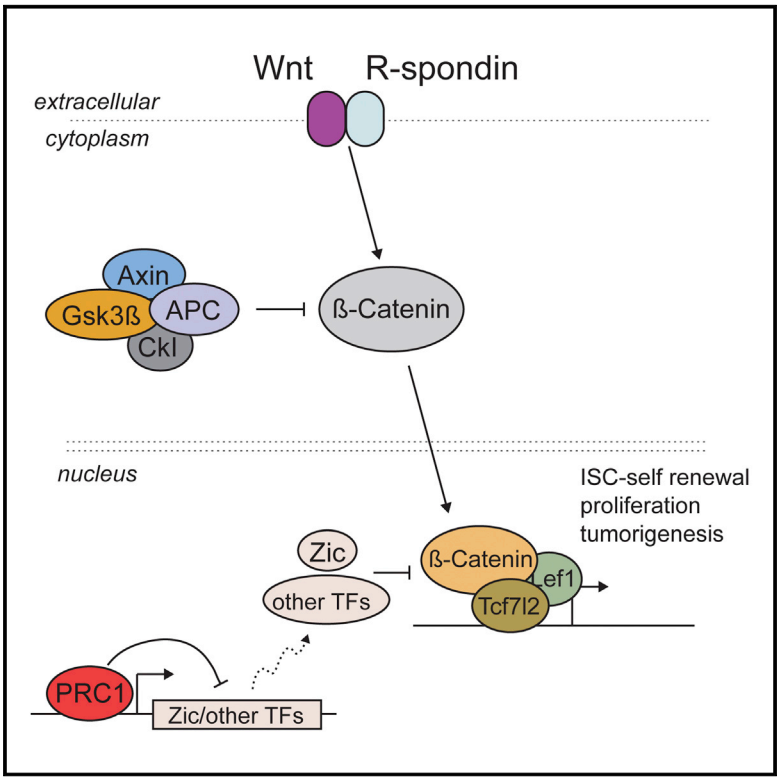

Authors

Fulvio Chiacchiera, Alessandra Rossi, SriGanesh Jammula, ..., Joerg Huelsken, Haruhiko Koseki, Diego Pasini

Correspondence

diego.pasini@ieo.eu

In Brief

Chiacchiera et al. show that PRC1 activity is essential to maintain integrity of the intestinal epithelium during homeostasis and in cancer. Mechanistically, PRC1 represses non-lineage-specific transcription factors that in turn directly affect β-catenin/Tcf transcriptional activity and Wnt-dependent intestinal stem cell self-renewal.

Highlights

- PRC1 activity controls the self-renewal of intestinal stem cells
- Intestinal identity is maintained by suppressing non-tissue-specific transcription
- Activated TFs directly interfere with nuclear β-catenin transcriptional activity
- Wnt/β-catenin signaling is sustained under normal and pathological conditions

Accession Numbers

GSE65322

Chiacchiera et al., 2016, Cell Stem Cell *18*, 91–103
January 7, 2016
http://dx.doi.org/10.1016/j.stem.2015.09.019

Cell Stem Cell
Article

Polycomb Complex PRC1 Preserves Intestinal Stem Cell Identity by Sustaining Wnt/β-Catenin Transcriptional Activity

Fulvio Chiacchiera,[1,4] Alessandra Rossi,[1,4] SriGanesh Jammula,[1] Andrea Piunti,[1] Andrea Scelfo,[1] Paloma Ordóñez-Morán,[2] Joerg Huelsken,[2] Haruhiko Koseki,[3] and Diego Pasini[1,*]
[1]Department of Experimental Oncology, European Institute of Oncology, Via Adamello 16, 20139 Milan, Italy
[2]École Polytechnique Fédérale de Lausanne (EPFL), ISREC, Lausanne CH-1015, Switzerland
[3]Developmental Genetics Group, RIKEN Research Centre for Allergy & Immunology (RCAI), 1-7-22 Suehiuro-cho, Tsurumi, Yokohama, Kanagawa 230-0045, Japan
[4]Co-first author
*Correspondence: diego.pasini@ieo.eu
http://dx.doi.org/10.1016/j.stem.2015.09.019

SUMMARY

Polycomb repressive complexes (PRCs) are among the most important gatekeepers of establishing and maintaining cell identity in metazoans. PRC1, which plays a dominant role in this context, executes its functions via multiple subcomplexes, which all contribute to H2AK119 mono-ubiquitination (H2Aubq). Despite our comprehensive knowledge of PRC1-dependent H2Aubq in embryonic stem cells and during early development, its role in adult stem cells still remains poorly characterized. Here we show that PRC1 activity is required for the integrity of the intestinal epithelium, regulating stem cell self-renewal via a cell-autonomous mechanism that is independent from *Cdkn2a* expression. By dissecting the PRC1-dependent transcription program in intestinal stem cells, we demonstrate that PRC1 represses a large number of non-lineage-specific transcription factors that directly affect β-catenin/Tcf transcriptional activity. Our data reveal that PRC1 preserves Wnt/β-catenin activity in adult stem cells to maintain intestinal homeostasis and supports tumor formation induced by the constitutive activation of this pathway.

INTRODUCTION

Adult tissues are maintained and constantly regenerated by the activity of tissue-specific multipotent stem cells. This reservoir is periodically activated and compensates for cell loss and tissue damage, while preserving the stem cell pool (Barker et al., 2010). Stem cell lineage commitment and their terminal differentiation is the outcome of a coordinated series of signaling events that converge on chromatin to regulate the establishment of lineage-specific transcription programs, where the chromatin environment and its modifications limit and support the activity of transcription factors (TF) by regulating their accessibility and by maintaining the established transcription programs.

Among the different chromatin modifiers, Polycomb group (PcG) proteins play a pivotal role in coordinating development, differentiation, and cell proliferation, in part by maintaining the repressed state of target genes by monoubiquitylating histone H2AK119 (H2Aubq) and by trimethylating histone H3K27 (H3K27me3) (Aloia et al., 2013). These modifications are controlled by the Polycomb repressive complexes 1 (PRC1) and 2 (PRC2), respectively, which localize together at CpG-rich transcription start sites (TSSs). PRC1 exists in at least five distinct complexes that all retain the Ring1a or Ring1b subunits that act as specific H2Aubq E3 ligases (Gao et al., 2012). Because PRC1 and PRC2 directly regulate the repression of a large set of common target genes, different models of functional dependency between these complexes have been proposed over the years (Gao et al., 2012; Scelfo et al., 2014) that suggest a dominant role for the PRC1 repressive activity (Blackledge et al., 2014; Cooper et al., 2014). Whereas Ring1a and Ring1b can be redundant during development (del Mar Lorente et al., 2000; Voncken et al., 2003), the Ring1a/b double KO embryos are impaired at the two-cell stage (Posfai et al., 2012), highlighting the requirement to inactivate both proteins to fully uncover PRC1 biological roles.

Despite the extensive literature on the role of PRC1 in regulating gene transcription, embryonic stem cell (ESC) differentiation, and development, the role of PRC1 activity in adult stem cells is still largely unexplored. Using genetic tools that fully inactivate H2Aubq deposition in adult mice, we have discovered that the Ring1a/b activity is essential for the homeostasis of the adult mouse intestine. The small intestine (SI) is one of the most dynamic adult tissues, with the highest renewal time among all solid organs (of 4–5 days). This high turnover is maintained by a pool of fast-cycling intestinal stem cells (ISCs) that reside at the bottom of the crypts of Lieberkuhn characterized by the high expression of the R-spondin receptor Lgr5 (Barker, 2014). These cells divide symmetrically, cycling once per day, generating actively proliferating, transient amplifying progenitors that gradually migrate toward the tip of the villi, differentiating as they go into absorptive or secretory cells that undergo apoptosis as soon as they reach the tip and then shed into the intestinal lumen (van der Flier and Clevers, 2009). The Wnt signaling plays a fundamental role for both ISC self-renewal and regeneration of the intestinal

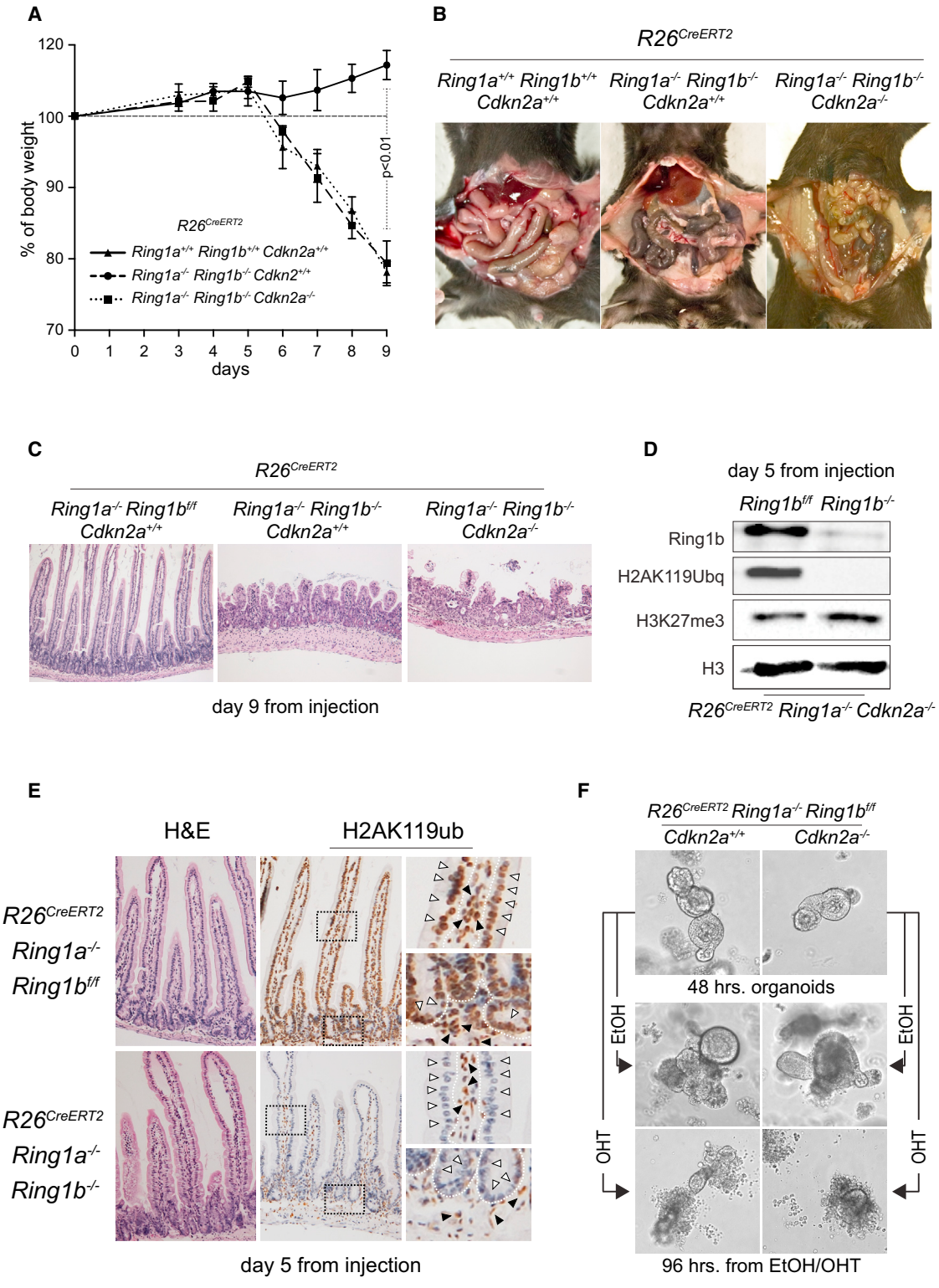

Figure 1. Global PRC1 Depletion Reveals a Role in Intestinal Homeostasis

(A) Body weight curves of the indicated *R26*^{CreERT2} mice injected with tamoxifen. (*R26*^{CreERT2} n = 10; *R26*^{CreERT2} *Ring1A*$^{-/-}$ *Ring1B*$^{-/-}$ n = 10; *R26*^{CreERT2} *Ring1A*$^{-/--}$ *Ring1B*$^{-/-}$*Cdkn2a*$^{-/-}$ n = 10).

(B) Autopsy of different *Rosa26*^{CreERT2} mice 9 days after injection.

(C) H&E staining of small intestinal sections from the indicated *R26*^{CreERT2} mice 9 days after injection with oil (left) or tamoxifen (middle and right).

(D) Western blot analysis of proteins extracted from crypts purified from the indicated *R26*^{CreERT2} mice 5 days after injection with oil (left) or tamoxifen (right).

(legend continued on next page)

epithelium, as its suppression leads to a loss of intestinal architecture and morbidity (Fevr et al., 2007; Korinek et al., 1998; van Es et al., 2012). In contrast, mutations that perturb β-catenin degradation, which preferentially occur on APC and β-catenin itself, lead to the expansion of the proliferative compartment and represent one of the hallmarks of familiar and sporadic intestinal tumors.

Here we have uncovered the fundamental role of PRC1-dependent transcriptional repression in maintaining ISC proprieties, providing a functional connection between PRC1 repression and Wnt-dependent transcriptional activity. Using ISC-specific *Ring1a/b* inactivation, our data genetically demonstrate mechanistic insight about how PRC1 acts as a positive regulator of ISC functions, thereby preserving epithelial integrity under physiological and pathological conditions.

RESULTS

PRC1 Activity Is Required for Intestinal Homeostasis Independently of *Cdkn2a* Repression

To uncover the functional proprieties of Ring1a and Ring1b (hereafter termed Ring1a/b)-dependent deposition of H2Aubq in adult tissues, we took advantage of a mouse model that couples a constitutive KO allele for *Ring1a* (*Ring1a*$^{-/-}$) and a Cre-dependent conditional KO (cKO) allele for *Ring1b* (*Ring1b*$^{f/f}$) (de Napoles et al., 2004) with the expression of a 4-hydroxytamoxifen (OHT)-inducible CreER^{T2} fusion that is constitutively expressed from the *Rosa26* locus (*R26*^{CreERT2}) in all adult tissues. The loss of Ring1a is fully compensated by Ring1b expression, as *Ring1a*$^{-/-}$ mice are viable and fertile, with only minor defects in the axial skeleton (del Mar Lorente et al., 2000). We therefore used this genetic model to acutely inactivate the activity of all PRC1 complexes in 8- to 12-week-old, sex-matched adult C57/B6 mice by intraperitoneal tamoxifen injections. We observed that *Ring1a/b* inactivation induced a rapid loss of body weight of up to 30% soon after the 9-day post-tamoxifen injection (pti, Figure 1A), coupled with a thinner intestine filled up with bloody feces (Figure 1B).

Because it is well established that Polycomb complexes are direct transcriptional repressors of the *Ink4a-Arf* (*Cdkn2a*) locus, and that p16 and Arf activation is a major mechanism behind different PcG-related loss-of-function phenotypes (Popov and Gil, 2010), we took advantage of an allele that constitutively inactivates p16 and Arf expression (*Cdkn2a*$^{-/-}$) (Serrano et al., 1996) to determine the dependency between PRC1 loss-of-function and *Cdkn2a* repression. These analyses revealed that both the loss of body weight and the impaired intestinal homeostasis were independent of p16 and Arf expression (Figures 1A and 1B). H&E staining of small and large intestine sections of *Cdkn2a*-proficient and -deficient mice confirmed that the intestines were functionally impaired, with a compromised crypt-to-villi architecture of the epithelium (Figures 1C and S1A). Western blot analysis of crypt preparations before the onset of this phenotype (5 days pti) confirmed that Ring1b expression was efficiently inactivated, and that no H2Aubq was deposited, upon loss of PRC1 activity (Figure 1D). This result was substantiated by immunohistochemical analyses showing that H2Aubq was actively deposited along the crypt-villus axis (including the stem cell compartment), and that acute inactivation of Ring1a/b activity rapidly impaired its deposition in all epithelial cells (Figure 1E). Importantly, loss of H2Aubq did not affect the global deposition of H3K27me3, showing that PRC1-dependent H2Aubq does not control PRC2 activity in this tissue and further underscoring the specific role of PRC1 in controlling intestinal homeostasis (Figure 1D). The other major organs, including spleen, lung, liver, kidney, and heart appeared grossly normal in *Ring1a/b* double KO mice (dKO) at the same days pti presented in Figures 1A and 1B (Figure S1B), suggesting a direct role of PRC1 in controlling intestinal homeostasis.

To confirm this observation, we isolated crypts before tamoxifen treatment and grew them in vitro as three-dimensional (3D) minigut organoids (Figure 1F). Organoids were allowed to form crypt-like structures for 48 hr before the *Ring1b*$^{f/f}$ conditional alleles were inactivated by addition of OHT to the culture media. This induced a rapid regression of minigut growth in both *Cdkn2a*-proficient and -deficient cells (Figure 1F), demonstrating that PRC1 activity is essential for sustaining intestinal homeostasis, independent of the local environment. This result was not an unspecific effect induced by OHT treatment, as *R26*^{CreERT2} *wild-type* (WT) organoids, cultured in the presence of OHT, were not compromised in development and growth (data not shown). Together, these data strongly suggest that PRC1 activity plays a direct role in the homeostasis of the adult intestinal epithelia.

PRC1 Regulates the Self-Renewal and Proliferation of Intestinal Stem Cells

To investigate the specific role of PRC1 in maintaining intestinal architecture, we took advantage of a knockin mouse model developed by the H. Clevers laboratory, in which the expression of both eGFP and CreER^{T2} is driven by the ISC-specific *Lgr5* promoter (*Lgr5*$^{GFP\text{-}CreERT2}$) (Barker et al., 2007). This model displays a non-uniform GFP and CreER^{T2} expression that, due to the clonal nature of adult intestinal crypts (Snippert et al., 2010), allows phenotypic analyses to be performed at a single-crypt level without affecting the overall functionality of the intestinal epithelium. We therefore used this model to characterize the role of PRC1 specifically in ISCs.

Immunostaining in these mice revealed the direct dependency between loss of Ring1b expression and lack of H2Aubq deposition at the single-crypt level and further confirmed that Ring1a/b are active in ISCs and compensate for each other (Figure 2A). Histological analysis performed at different days pti on intestinal sections from Ring1a/b dKO mice revealed the presence of degenerating crypts starting from 7 days pti. The number of these abnormal crypts increased after 15 day and then gradually

(E) H&E and immunostaining using anti-H2AK119ubq on intestinal sections prepared from mice 5 days after injection with oil (top) or tamoxifen (bottom). White arrowheads highlight epithelial cell nuclei, and black arrowheads, lamina propria–associated nuclei.
(F) Minigut cultures obtained from purified small intestinal crypts of *R26*^{CreERT2} mice carrying the indicated genotypes. The purified crypts were split in two and separately cultured for 48 hr. The formed miniguts were either treated with OHT, to activate CRE recombinase, or EtOH as control.
Related to Figure S1.

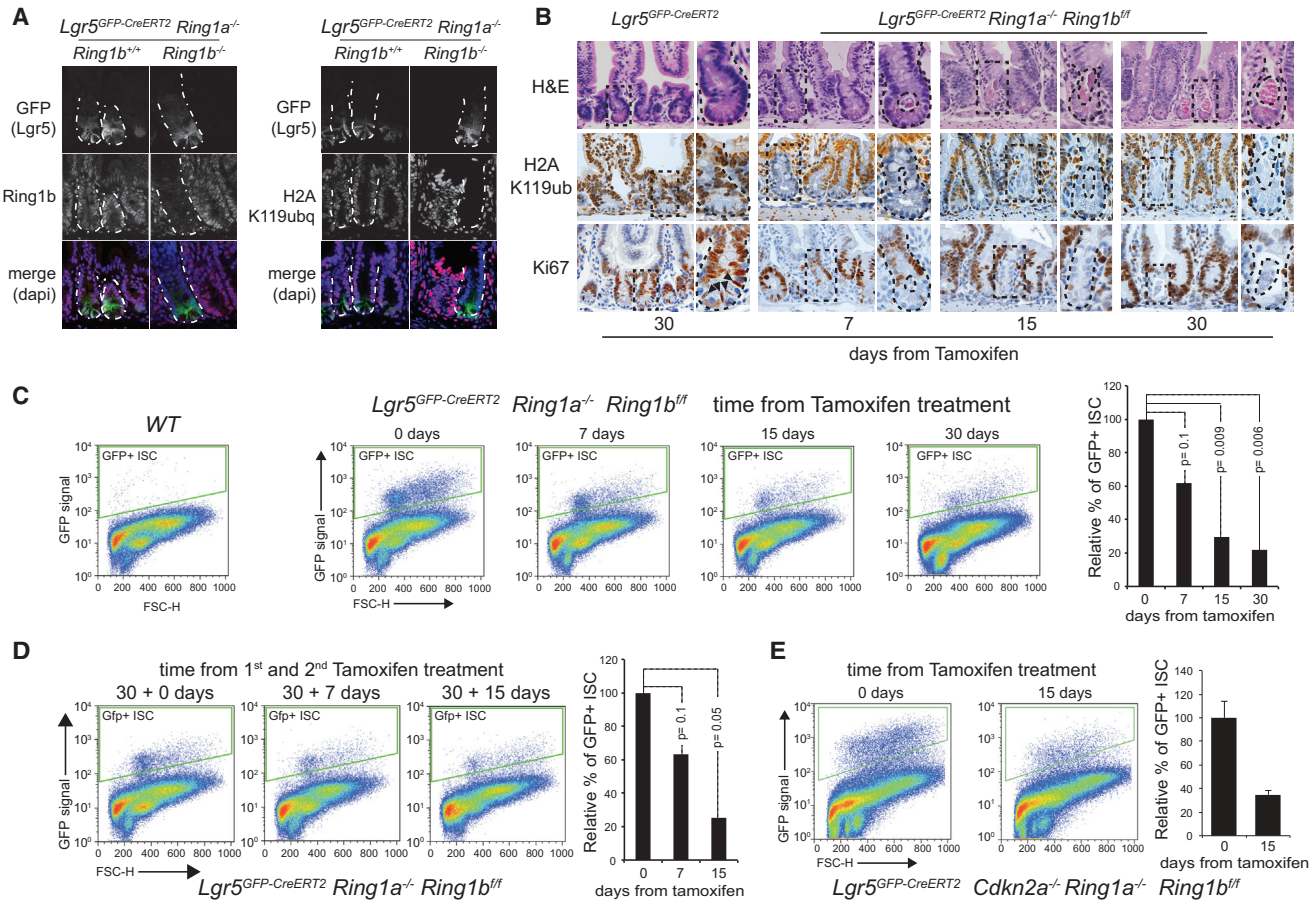

Figure 2. Intestinal Stem Cell–Specific PRC1 Ablation Affects Normal Crypt Architecture and Reduces Intestinal Stem Cell Number

(A) Immunostaining of near-native small intestine sections for the indicated *LGR5*$^{GFP\text{-}CreERT2}$ mice at 7 days after tamoxifen injection. GFP-positive crypts are highlighted (dashed line).

(B) Histological and immunohistochemical examination of small intestinal sections from WT and *Ring1a*$^{-/-}$ *Ring1b*$^{-/-}$ *LGR5*$^{GFP\text{-}CreERT2}$ mice at different times after tamoxifen injection. Proliferating stem cells at crypt base (arrowheads) and mucopolysaccharides accumulated at the luminal side of the crypts (dashed line).

(C and D) FACS analysis and quantification (n = 7) of GFP-positive ISCs at different times after tamoxifen injection in *Cdkn2a*$^{+/+}$ (C) and *Cdkn2a*$^{-/-}$ (D) mice (n = 4). The p values were determined by Wilcoxon non-parametric statistical test.

(E) FACS analysis quantification (n = 2) of GFP-positive cells after a second round of tamoxifen administration. Thirty days after the first tamoxifen injection, mice were subjected to a second round of tamoxifen administration. The number of GFP-positive cells was analyzed at 7 and 15 days after the second administration. p values were determined by Wilcoxon non-parametric statistical test.

Related to Figure S2.

decreased by negative selection (Figure S2B). Degenerating crypts appeared to be shrinking cystic crypts filled by eosinophilic debris with PAS-positive mucus (Figures S2A and S2B) and composed by a lower number of cells (Figures 2B and S2A). All these crypts negatively stained for H2Aubq (Figures 2B, S2A, and S2B) and showed a gradual reduction of Ki67-positive proliferating cells, starting from the bottom of the crypts and expanding to the transient amplifying compartment (Figure 2B). Degenerating crypts gradually disappeared and after 60 days pti, the intestinal epithelium appeared normal (Figure S2C). Loss of crypt architecture was not due to enhanced cell death, as no increase in the number of apoptotic cells was observed between H2Aubq-positive and -negative crypts by TUNEL assays (Figure S2D). The efficiency of TUNEL staining was measured by detecting the apoptotic cells that are physiologically present at the tip of the small intestinal villi (Figure S2D). Overall, these results suggest that the specific loss of PRC1 activity in ISCs affects crypt homeostasis without inducing cell death.

To further characterize whether *Ring1a/b* was required for ISC maintenance, we analyzed disaggregated crypt preparations by fluorescence-activated cell sorting (FACS) at different time points pti to quantify the pool of GFP+ stem cells over time. This analysis showed a remarkable reduction of GFP+ ISCs, that approaches 80% after 30 days pti (Figure 2C). As neither tamoxifen exposure of *Ring1a/b* WT mice, nor single loss of *Ring1a* expression, induced a significant reduction of GFP+ ISC (Figure S2E), this result demonstrated that loss of PRC1 activity leads to a strong reduction of the ISC pool in vivo. We then analyzed FACS staining for Ring1b and H2Aubq; the specificity of this was validated using *Ring1a/b* dKO mouse embryonic fibroblasts; (Figure S2F) (Piunti et al., 2014). This FACS staining confirmed that PRC1 activity was efficiently inactivated in the

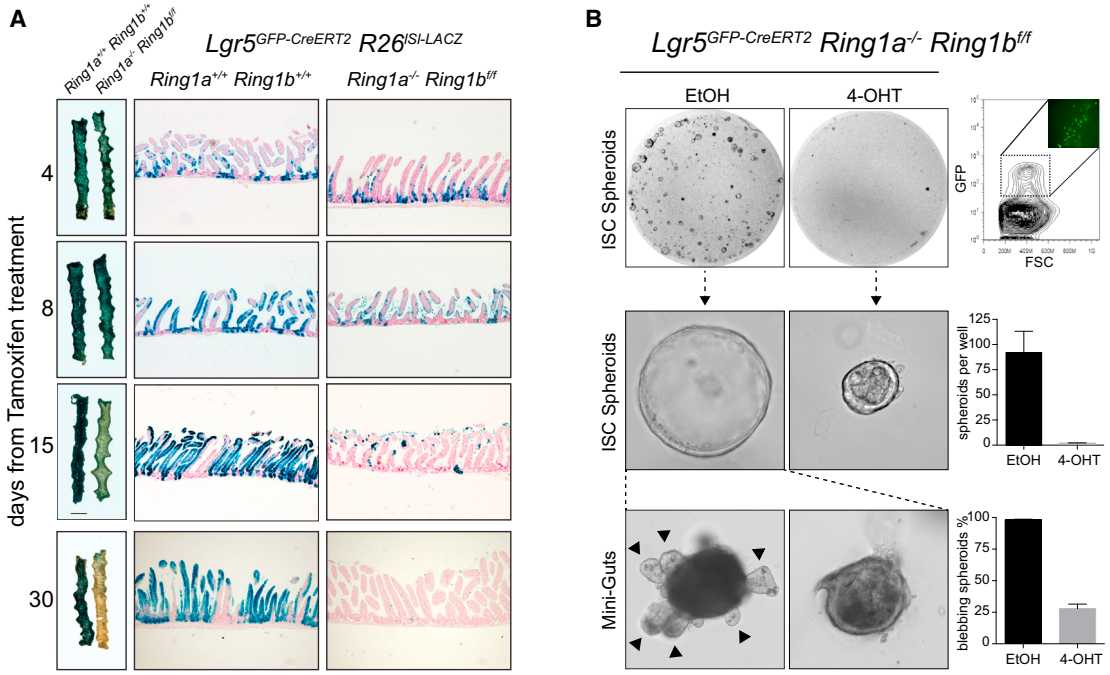

Figure 3. PRC1 is Required for ISC Maintenance in a Cell-Autonomous Manner

(A) In vivo ISC lineage tracing. R26$^{lsl\text{-}LACZ}$ mice with the indicated genotypes were injected with tamoxifen and sacrificed at the indicated time points. For each time point, the small intestine from *wild-type* and *Ring1a*$^{-/-}$ *Ring1b*$^{-/-}$ mice were stained with X-GAL. The whole-stained samples and the relative sections are shown. Nuclei were counterstained using Nuclear Fast Red.

(B) FACS-sorted ISCs from *LGR5*$^{GFP\text{-}CreERT2}$ *Ring1a*$^{-/-}$ *Ring1b*$^{f/f}$ mice were cultured in vitro in the presence of Wnt3a and exposed to either OHT or EtOH as a control. The number of spheroids obtained in each well was scored. The spheroids obtained from the EtOH treated sample were further cultured in the absence of Wnt3a and in the presence of either OHT or EtOH to assay their ability to form crypt-like structure (arrowheads). The percentage of "blebbing" spheroids was scored. Representative images of three replicates are shown.

Related to Figure S3.

GFP+ stem cells, and that loss of Ring1a/b activity was rapidly counterselected in the remaining GFP+ stem cell population, which retained normal Ring1b and H2Aubq levels after 30 days pti (Figures S2G and S2H). Indeed, a second exposure to tamoxifen at this time point further exhausted the remaining pool of GFP+ ISCs, confirming that *Ring1a/b* dKO ISCs are counterselected by WT GFP+ cells that did not inactivated the *Ring1b* conditional allele after the first tamoxifen treatment (Figure 2D). Finally, consistent with our previous results (Figure 1), loss of PRC1 activity in *Cdkn2a*$^{-/-}$ ISCs also resulted in a strong reduction of the GFP+ ISC pool (Figure 2E), further confirming that PRC1 works independently from *Cdkn2a* repression in controlling stem cell functions and crypt homeostasis.

To further characterize the role of PRC1 in maintaining ISC functions, we introduced a tracing allele that expresses LacZ from the *Rosa26* locus under the control of a stop cassette that can be excised by Cre-recombinase activation (*R26*$^{lsl/LacZ}$) (Soriano, 1999). This allowed us to label ISCs with constitutive LacZ expression, introducing a heritable genetic mark that is transmitted to the entire progeny of epithelial cells. Upon tamoxifen administration, a similar number of ISCs had LacZ expression in both *Ring1a/b*-proficient and -deficient animals (4 days pti, Figure 3A). However, while the LacZ-positive ISCs in WT mice were able to maintain all lineages of the intestinal epithelium, those in *Ring1a/b* dKO mice were unable to sustain crypt homeostasis, and LacZ-positive cells completely disappeared from the epithelium within 30-days pti (Figure 3A). Similar results were also observed in Lgr5+ colonic and pyloric stem cells suggesting a conserved role of PRC1 in maintaining Lgr5+ stem cells in the entire gastro-intestinal tract (Figures S3A and S3B). Taken together, these results demonstrate the essential role of PRC1 in maintaining intestinal homeostasis by sustaining the self-renewing capacity of the ISC pool.

To obtain more direct evidence that loss of Ring1a/b activity compromises the self-renewal and proliferation of stem cells, we isolated GFP+ ISCs by FACS sorting and allowed them to grow as undifferentiated spheroids in a Wnt3a-conditioned medium, to expand the stem cell population (Sato et al., 2011). Under these conditions, normal ISC efficiently form and maintain large spheroids; however, ISC-specific inactivation of *Ring1a/b* (by OHT addition to the culture media) fully prevented the stem cells from proliferating in vitro (Figure 3B top and middle images). Moreover, in agreement with the results presented in Figure 1F, inactivation of Ring1a/b in fully formed spheroids failed to sustain minigut cultures, as evidenced by the absence of crypt-like structures that normally form upon Wnt3a removal (Figure 3B, bottom images). Together, these results demonstrate the essential role of PRC1 activity in preserving the homeostasis of the adult intestinal epithelium by promoting ISC self-renewal independently from their niche.

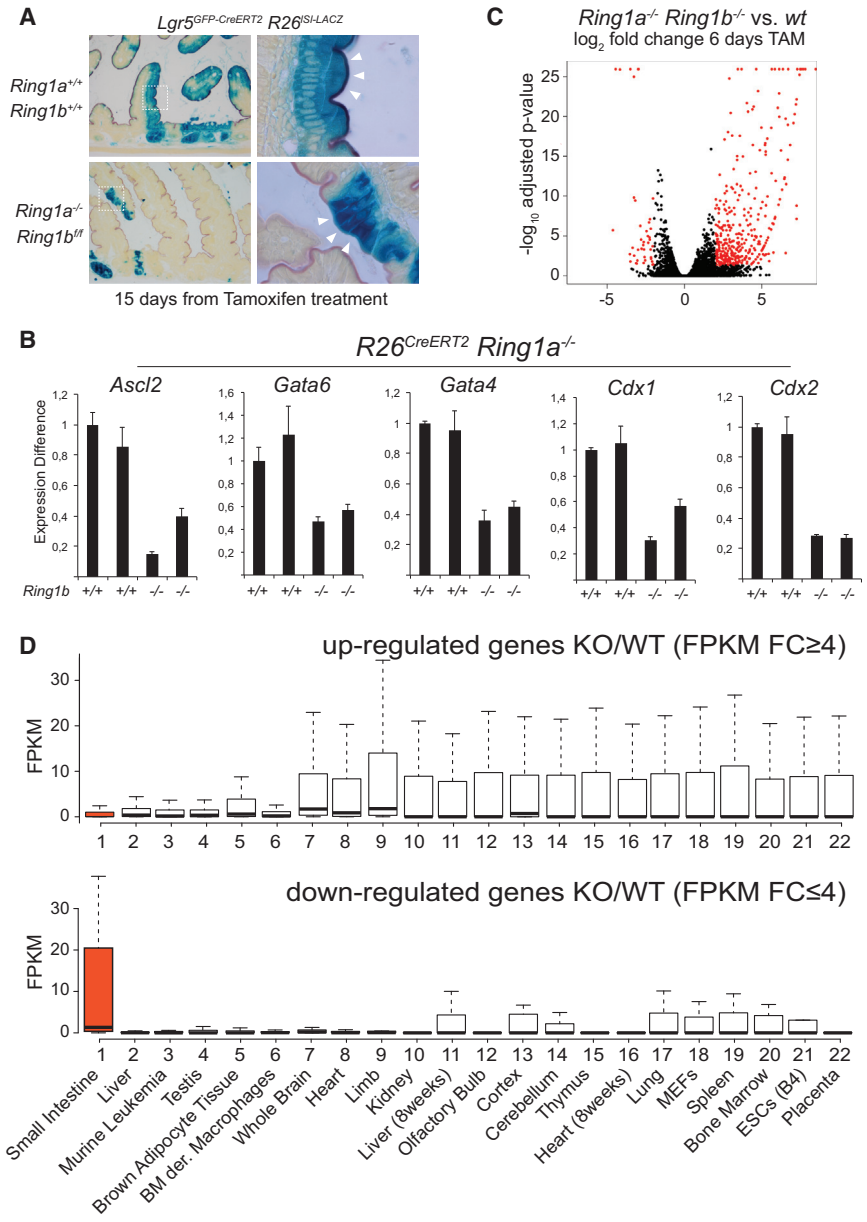

Figure 4. Inactivation of PRC1 Activity in ISCs Triggers Loss of Lineage Identity

(A) Enterocytes differentiation of cells derived from wild-type and mutant PRC1 null ISCs. Alkaline phosphatase activity were reveal using intestinal sections derived from $R26^{lSl\text{-}LACZ}$ wild-type and $Ring1a^{-/-}$ $Ring1b^{-/-}$.

(B) Expression of intestinal-specific transcription factors in wild-type and $Ring1A^{-/-}$ $Ring1B^{-/-}$crypts.

(C) Volcano plot depicting the genome-wide expression changes between $Ring1a^{-/-}$ $Ring1b^{-/-}$ and *wild-type* ISCs purified from the indicated $Lgr5^{GFP\text{-}CreERT2}$ mice at 6 days after tamoxifen injection. Differentially regulated genes were defined by a minimum fold change difference of 4 and an adjusted $p \leq 0.05$.

(D) Box plots representing the expression levels of the significantly up- and downregulated genes presented in (C) in the different tissues.

Related to Figure S4.

PRC1 Directly Ensures the Maintenance of Intestinal Identity in the Stem Cells

To investigate whether PRC1 deficient ISCs develop into a normally differentiated progeny, we taken advantage of $R26^{lSlLacZ}$ mice to analyze the activity of intestinal alkaline phosphatase (Alpi), which is a marker of the most abundant differentiated cells type in the villi, the enterocytes. As shown in Figure 4A, the fewer cells located in the villus compartment derived from *Ring1a/b* dKO ISCs did not express alkaline phosphatase suggesting an impairment in ful differentiation into specialized intestinal epithelial cells. Consistent with this, the expression of transcription factors specifically involved in the differentiation of specialized intestinal cells was reduced in *Ring1a/b* dKOs (Figure 4B). To gain insight into this apparent loss of cell identity, we decided to characterize the transcriptional program controlled by PRC1 in ISCs. FACS-sorted GFP+ ISCs from the small intestine of WT and *Ring1a/b* dKO $Lgr5^{CreERT2}$ mice at 6 days pti were used to purify total mRNA. To minimize the contamination of the isolated ISC pools with ISC:Paneth cell doublets, we adopted a "gating" strategy that allowed us to exclude GFP+/$Cd24^{high}$ double-positive events, to isolate highly pure ISC populations (Figures S4A–S4F). The inactivation efficiency of *Ring1a/b* alleles was first determined by real-time qPCR expression analyses (Figure S4G) and further validated by western blotting (Figure S4H). These cells were used to delineate the global transcriptional changes with RNA-sequencing (RNA-seq) analysis (Table S1). Consistent with the repressive nature of PRC1, we observed a preferential activation of gene expression in *Ring1a/b* dKO as compared to WT ISCs (Figure 4C). Using a 4-fold cutoff to define the differentially regulated genes (DRG), we observed an ~9:1 ratio between the number of significantly upregulated (376) and downregulated (42) genes in *Ring1a/b* dKO stem cells (red dots, Figure 4C). To investigate whether loss of PRC1 activity forced ISCs to adopt a specific differentiation program, we compared both up- and downregulated genes with the transcriptional profiles obtained from different tissues. The global expression levels of the group of upregulated genes revealed that loss of PRC1 transcriptional control induced the expression of large set of genes that did not belong to the intestinal lineage (Figures 4D and S4I). These genes were fully silent in whole intestine but expressed at high levels in several other tissues. real-time qPCR analyses confirmed the RNA-seq analysis showing upregulation of these genes in *Ring1a/b* dKO crypts (Figure S4L). In contrast, the expression of the downregulated genes was specifically elevated in the small intestine with

respect to other tissues (Figure 4D) according to what was observed in *Ring1a/b* dKO crypts (Figure 4B). Together, these results suggest that PRC1 inactivation leads to a general loss of intestinal lineage identity rather than to premature differentiation of ISCs.

To determine to which extent these transcriptional changes are a direct consequence of PRC1-dependent repression, we analyzed Ring1b and H2Aubq by chromatin immunoprecipitation sequencing (ChIP-seq) in formaldehyde-fixed chromatin preparations from both crypts and ISCs from *Lgr5*^{CreERT2} WT mice. The purity of the crypt preparations was confirmed by the specific enrichment of ISC and Paneth cell markers, and by the exclusion of markers expressed by the most representative differentiated cells of the villi and stromal cells (Figure S5A). The GFP+ ISCs were instead purified following the same approach presented in Figure S4. These analyses identified several Ring1b- and H2Aubq-enriched genomic loci in both crypts and ISCs (Table S2). As expected, Ring1b binding fully overlapped with H2Aubq, which displays a broader deposition (Figure S5B). This analysis also identified a larger number of Ring1b- and H2Aubq-enriched genomic loci in crypts with respect to ISCs, suggesting a more diffused activity of PRC1 in progenitor cells. However, Ring1b occupancy and the deposition of H2Aubq detected in ISCs were fully conserved in intestinal crypts and villi (Figures S5C–S5E; Tables S2 and S3). Moreover, RNA-seq analysis performed with the *Ring1a/b* dKO villi fraction confirmed that PRC1 is required to maintained transcriptional repression of a defined set of target genes that do not change along the crypt-villus axis (Figures S5F and S5G; Table S4), suggesting that PRC1-dependent lineage identity is established at stem cell level and does not change significantly in progenitor and differentiated cells. Importantly, PRC1 activity was specifically enriched at the promoter of genes that were transcriptionally activated in *Ring1a/b* dKO ISCs (Figures 5A and 5B). This direct correlation is almost complete when only fully silent genes in WT ISCs (FPKM $\leq$0.05) were taken into consideration in this analysis (Figure 5B). Thus, PRC1 activity directly maintains transcriptional repression of almost all the identified upregulated genes. Overall, these data define the direct transcriptional circuits of PRC1 in ISCs and highlight the diffuse repressive activity of PRC1 in these cells.

PRC1-Repressed Transcription Factors Directly Inhibit β-Catenin/Tcf7l2 Transcriptional Activity

To characterize the molecular mechanisms by which PRC1 activity could sustains ISC self-renewal and proliferation, we interrogated gene ontology databases to unveil functional proprieties among the group of upregulated genes. This analysis identified a massive activation of DNA-binding TFs in *Ring1a/b* dKO ISCs (Figure 5C). Importantly, this was the only functional ontology class that was significantly enriched within our signature of upregulated genes, suggesting that the main function of PRC1 activity is to suppress the transcription of these genes in ISCs. Interestingly, several of these factors have been reported to interfere directly with the transcriptional activity of the β-catenin/Tcf complex in different cellular settings (Fujimi et al., 2012; Ito et al., 2008; Jung et al., 2004, 2005; Pourebrahim et al., 2011; Sinner et al., 2007). This is a central activity for the self-renewal and proliferation of ISCs that controls the homeostasis of the entire intestinal epithelium (Korinek et al., 1998; van Es et al., 2012). Among these factors, we focused our attention on the Zic family of zinc finger TFs, which were previously shown to suppress β-catenin-induced axis duplication in *Xenopus* embryos (Fujimi et al., 2012; Pourebrahim et al., 2011). The genomic snapshots presented in Figure 5D highlight the transcriptional activation of different Zic genes in *Ring1a/b* dKO ISCs and the direct association of PRC1 activity to their promoters. Zic transcriptional activation was also confirmed with independent preparations of ISCs by real-time qPCR expression analyses (Figure 5E) and further validated in *Ring1a/b* dKO whole-crypt preparations using *R26*^{CreERT2} mice (Figure 5F). The specificity of Ring1b binding and the loss of H2Aubq deposition were confirmed by specific ChIP analyses at the *Zic1-5* promoters using chromatin prepared from WT compared to *Ring1a/b* dKO purified crypts (Figures S5H and S5I). Importantly, western blots from both ISCs and crypt extracts validated that Zic2 is overexpressed at the protein level (Figures 5G and 5H). This result further demonstrates the lack of expression of Zic2 in WT ISCs and confirms an effective protein accumulation of these TFs upon loss of PRC1-dependent transcriptional repression.

Considering the potential role of these TFs to interfere with Wnt-dependent transcriptional activity, our data suggest that the extensive upregulation of several DNA binding factors, such as the Zic proteins, in the absence of PRC1 repressive activity could interfere with the transcriptional activity of the β-catenin/Tcf7l2 complex. To test this hypothesis, we evaluated the expression of the five different *ZIC* TFs in six colorectal cancer cell lines. While APC mutant microsatellite-stable cell lines expressed very low or nondetectable levels for these genes, APC wild-type microsatellite-unstable cells expressed detectable levels of ZIC1, ZIC2, and ZIC5 (Figure S6A). To test the effect of ZICs ectopic expression on WNT transcriptional activity, we cloned and independently expressed Flag-tagged ZIC1 and ZIC2 in SW480 colorectal cancer cell line and found by immunoprecipitation that both ectopically expressed ZIC1 and ZIC2 interacted efficiently with endogenous TCF7L2 (also known as TCF4, Figures 6A and 6B). More importantly, this interaction correlated with the ability of ZIC1 or ZIC2 to suppress TCF-dependent luciferase transcription from a TCF-responsive promoter in a dose-dependent manner (TOP/FOP assays, Figure 6C) and by inhibiting the expression of physiological downstream targets of the WNT pathway in the same cells (Figure 6D). Consistent with this, simultaneous inhibition of ZIC1 and ZIC2 expression in HCT116 by shRNAs expression enhanced β-CATENIN/TCF transcriptional activity as shown by both the TOP/FOP assay and by the increased expression of the physiological targets EPHB3 and MYC (Figure S6B).

To finally show that ZIC protein expression is sufficient to impair intestinal homeostasis similarly to PRC1 loss of function, we cloned ZIC1 and ZIC2 coding sequences in an inducible CMV-driven lentiviral vector downstream to a lox-RFP-lox stop cassette and transduced *R26*^{CreERT2}-derived organoids (Figure 6F). Consistent with our data, the independent expression of either ZIC1 or ZIC2 by treatment of RFP-positive organoids with 4-OHT, induced organoids regression similarly to loss of PRC1 activity (Figures 6G and 6H). Together, these results strongly suggest that ZIC1 or ZIC2 expression inhibits the transcriptional activity of β-CATENIN/TCF, possibly via a direct

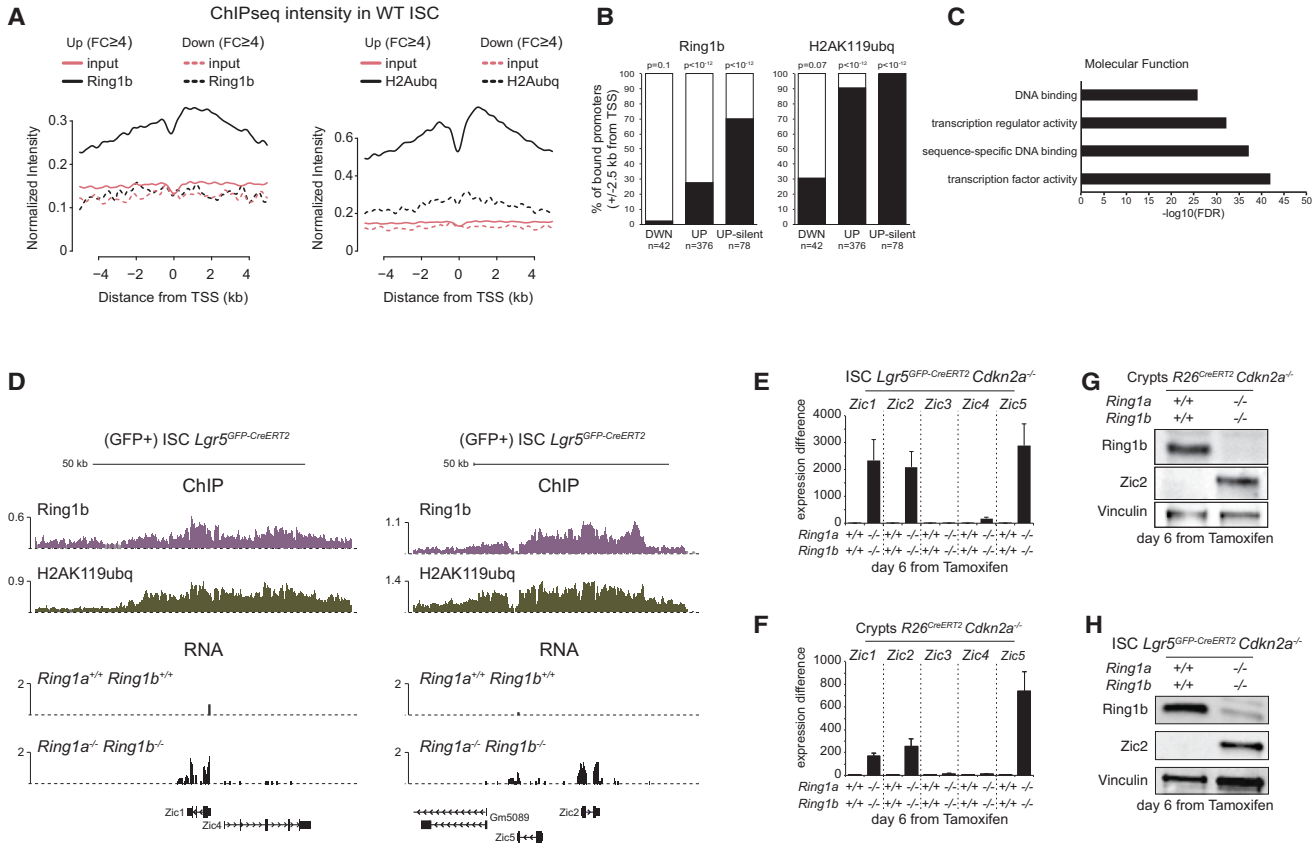

Figure 5. Loss of PRC1 Activity in the ISCs Induces Global Activation of DNA Binding Transcription Factors

(A) Average Ring1b and H2AK119Ubq ChIP-seq profile performed on ISCs purified from *Lgr5*$^{GFP\text{-}CreERT2}$ mice and centered around the TSS of either up- or downregulated genes defined in Figure 4.

(B) Bar plots showing the proportion of promoters directly occupied by Ring1b or H2AK119Ubq among differentially expressed genes defined in Figure 4. DWN indicates all downregulated genes; UP, all upregulated genes; and UP-silent, all upregulated genes with a basal expression in WT ISCs lower than 0.5 FPKM.

(C) GO analysis displaying the significantly enriched molecular functions in the group of upregulated genes.

(D) Genomic snapshots of the different *Zic* gene loci showing Ring1b and H2AUbq ChIP-seq results together with the RNA-seq data obtained from WT and *Ring1a*$^{-/-}$ *Ring1b*$^{-/-}$ ISCs at 6 days after tamoxifen injection.

(E and F) *Zic1-5* expression determined by real-time qPCR analyses of RNA purified from intestinal crypts from the indicated *R26*^{CreERT2} mice (F) or from ISCs purified from the indicated *Lgr5*$^{GFP\text{-}CreERT2}$ mice (E) both at 6 days after tamoxifen injection. *Tbp* expression was used as a normalizing control. Data represent mean ± SEM.

(G and H) Western blot analysis with Ring1B- and Zic2-specific antibodies of proteins extracted from intestinal crypts from the indicated *R26*^{CreERT2} mice (G) or from ISCs purified from the indicated *Lgr5*$^{GFP\text{-}CreERT2}$ mice (H), both at 6 days after tamoxifen injection. Vinculin was used as a loading control.

Related to Figure S5.

interaction with this complex, directly affecting tissue homeostasis in primary intestinal organoids.

These results allow us to envision a model in which loss of PRC1 repression induces a general upregulation of DNA-binding TFs that retain the ability to directly interact with the β-catenin/Tcf7l2 complex to inhibit its transcriptional activity. Consistently, Wnt/β-catenin signaling scored as the most affected pathway after the loss of PRC1 activity in ISCs (Figure S6C) and the expression of two canonical Wnt targets, EphB2 and EphB3, was abolished in PRC1-null crypts (Figure S6D). Indeed, the number of genomic sites enriched in Tcf7l2 binding (peaks) and the cumulative Tcf7l2 ChIP-seq signal were strongly reduced upon loss of PRC1 activity (Figures 7A–7D and Table S5), despite the levels of both Tcf7l2 and Ctnnb1 remain unchanged (Figure S6E). Tcf7l2 chromatin displacement was also observed in *Ring1a/b* dKO crypts (Figures 7A and S7A–S7D) accompanied by a destabilization of β-catenin and Tcf7l2 levels (Figure S6F; Table S5). The specificity of Tcf7l2 genomic association was confirmed by the strong prediction of the known Tcf7l2 DNA binding motif at the summit of the identified peaks in WT cells (Figure S7C). Together, these data demonstrate that loss of PRC1 activity induces a global displacement the β-catenin/Tcf7l2 complex from genomic DNA directly in ISCs.

PRC1 Activity Is Essential for β-Catenin Oncogenic Activity In Vivo

Our findings strongly suggest that the activity of the β-catenin/Tcf7l2 complex is compromised by the loss of PRC1 repressive control by a mechanism that acts downstream of β-catenin stabilization and nuclear localization. To provide further in vivo proof

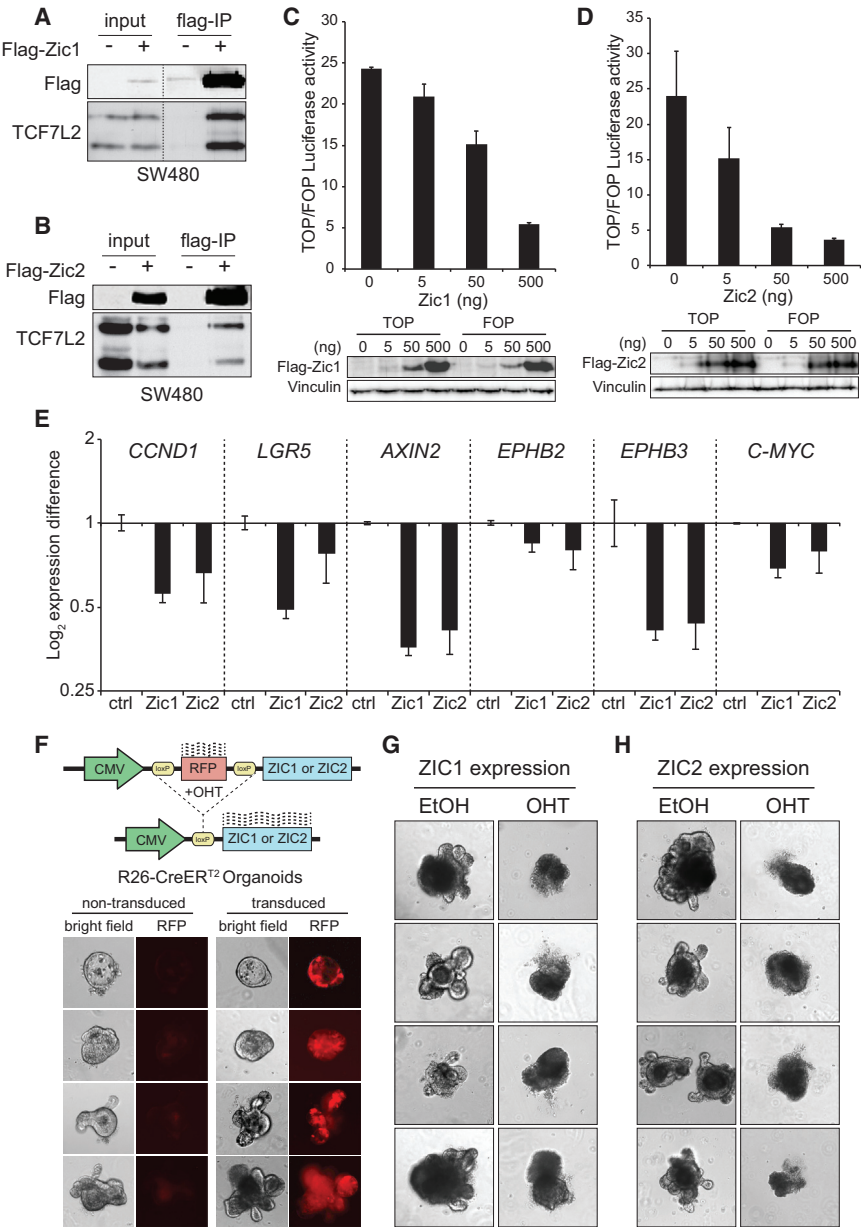

Figure 6. ZIC Proteins Directly Inhibit β-Catenin Transcriptional Activity

(A and B) Coimmunoprecipitation experiments between ectopically expressed Flag-tagged ZIC1 (A) or ZIC2 (B) with endogenous TCF7L2 in SW480 colon cancer cells.

(C and D) TOP/FOP Flash luciferase assay in SW480 cells transfected with increasing amount of ZIC1 (C) or ZIC2 (D) (n = 3). Immunoblots from the same protein extracts are shown to verify ZIC1 and ZIC2 expression. Vinculin served as a loading control.

(E) Expression difference determined by real-time qPCR analyses of RNA purified from SW480 cells infected with ZIC1 or ZIC2 lentiviral expression constructs for the indicated WNT/β-catenin endogenous targets. 18S expression was used as a normalizing control. Data represent mean ± SEM.

(F) Ectopic expression of Zic1 and Zic2 in intestinal crypt-derived organoids. Disaggregated *R26*^{CreERT2} derived crypts were infected with Cre inducible lox-RFP-lox constructs expressing either Zic1 or Zic2 and in vitro cultured. RFP+ organoids were cultured for 7 days, disaggregated, and allowed to reform. After approximately 4 days, RFP+ organoids were treated with 4-OHT to induce Zic1 (G) or Zic2 (H) expression or vehicle alone (EtOH). Pictures were taken after 3 days.

Related to Figure S6.

for this model, we used a genetic tool that constitutively activates β-catenin in vivo by Cre-mediated deletion of *Ctnnb1* exon 3 (*Ctnnb1*$^{ex3/ex3}$). Loss of exon 3 removes the GSK3β phosphorylation sites from Ctnnb1 that positively regulate β-catenin degradation leading to a constitutively stable β-catenin mutant. β-catenin stabilization in ISCs resulted in hyperplasia and massive adenoma formation in the entire small intestine (Harada et al., 1999) mimicking in mice the mutations that are found in sporadic and hereditary non-polyposis colorectal cancer (Johnson et al., 2005; Morin et al., 1997). Thus, we combined the *Ctnnb1*^{ex3} allele with conditional loss of Ring1a/b activity using ISC-specific *Lgr5*^{CreERT2}-mediated Cre inactivation. Indeed, stabilization of β-catenin in ISCs after tamoxifen treatment induced the enlargement of the mouse SI due to a massive formation of intestinal adenomas (Figure 7E, left images). However, the activation of β-catenin combined with loss of PRC1 activity in ISCs fully inhibited the ability of β-catenin to induce epithelial hyperplasia and tumor formation (Figure 7E, right images). Transcriptional analysis performed in ISCs purified from Ctnn1b$^{ex3/ex3}$ mice at 6 days pti confirmed that loss of PRC1 activity activates a very similar gene signature with respect to normal ISCs (Figures S7E and S7F; Table S6). To exclude the possibility that inhibition of adenoma formation in *Ring1a/b* dKO Ctnn1b$^{ex3/ex3}$ mice was due to ISCs exhaustion before addiction to a constitutive WNT activation, we took advantage of ''escaper'' tumors that can be found after 30 days pti in *Ring1a/b* dKO Ctnn1b$^{ex3/ex3}$ mice. These adenomas probably formed because of limited activity of CRE that recombined Ctnn1b$^{ex3/ex3}$ but not the Ring1b$^{fl/fl}$ allele as shown by the presence of both stabilized Ctnnb1 and H2Aubq deposition (Figure S7G). These rare events are positively selected and allowed us to inactivate *Ring1b* in Lgr5+ cells within adenomas established by constitutive WNT activation. Indeed, a second treatment with tamoxifen after 30 days strongly reduced the adenoma-associated Lgr5+ stem cells as shown by both ex-vivo fluorescent imaging on isolated small intestinal samples (Figure 7F) and by confocal microscopy on near-native sections (Figure S7H). These results were further confirmed in 3D cultures dependent by constitutive oncogenic β-Catenin activation. First we have generated organoids from ''escaper'' adenomas from

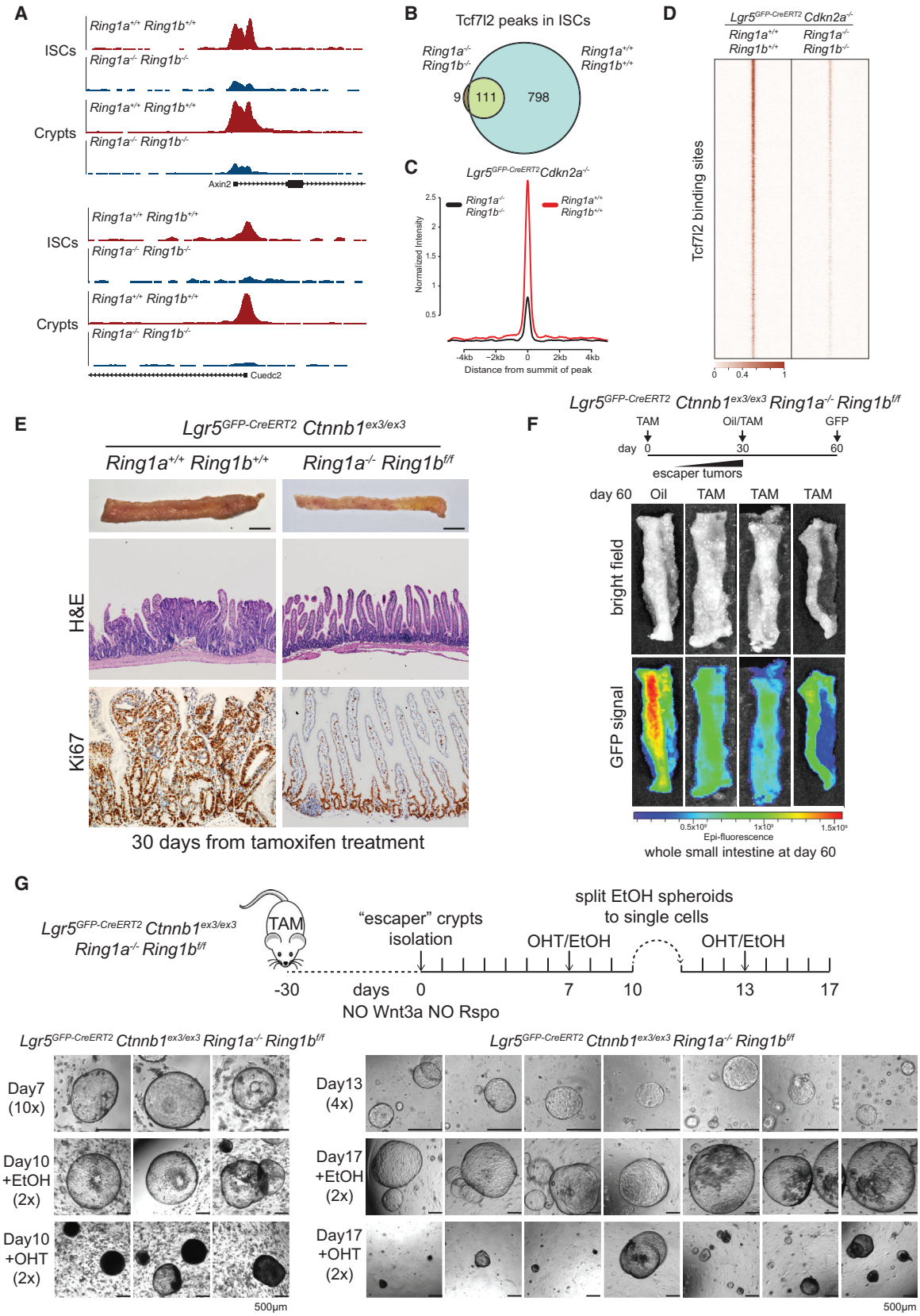

(legend on next page)

Ring1a/b dKO Ctnn1b$^{ex3/ex3}$ mice 30 days from the first tamoxifen treatment directly in the absence of RSPO1 and Wnt3a stimulation in the culture medium (Figure 7G). Second, we generated organoids from *R26*^{CreERT2} *Ring1b*$^{-/-}$ *Ring1b*$^{f/f}$ crypts, transduced them with lentiviruses expressing a constitutively active form of β-Catenin and selected for growth as spherical cysts in absence of of RSPO1 and Wnt3a stimulation (Figure S7I). In both cases, inactivation *Ring1b* by 4-OHT treatments induced the regression of oncogenic Ctnnb1 expressing spheroids. Together, these data genetically demonstrate that PRC1 activity is essential for β-catenin oncogenic activity downstream to its constitutive activation. We therefore propose a model in which PRC1 activity supports Wnt signaling and intestinal homeostasis by transcriptionally repressing direct negative regulators of β-catenin transcriptional activity.

DISCUSSION

The role of PcG proteins in regulating adult tissue homeostasis still remains quite elusive. This also includes the role of PRC1 and its dependent deposition of H2Aubq. The large majority of the current studies only determined the role of different components of the canonical PRC1 complex without fully addressing the general requirements of Ring1a/b-dependent H2Aubq deposition in adult tissues (Endoh et al., 2012). We have now identified a novel role of PRC1 activity in adult organisms: PRC1 activity is essential in regulating the homeostasis of the intestinal epithelium. By inactivating the catalytic subunits *Ring1a* and *Ring1b* that are shared among all different PRC1 subcomplexes specifically in Lgr5+ ISCs, we have further shown that PRC1 activity is required for stem cell self-renewal both in vivo and in vitro.

We show here that H3K27me3 is not affected by loss of H2Aubq deposition. Recent reports have demonstrated that PRC2 can bind directly H2Aubq in vitro (Kalb et al., 2014), and that PRC2 recruitment and H3K27me3 deposition are partially dependent on PRC1 activity in ESCs (Blackledge et al., 2014), fitting a model in which PRC2 recruitment and activity requires PRC1-dependent H2Aubq deposition at target sites. Importantly, our results suggest that this effect is cell-type specific rather than general, and that it can be regulated by multiple mechanisms—which are likely determined in a context-dependent manner—for stabilizing PRC1 and PRC2 complexes at chromatin. Overall, these data emphasize a dominant role of PRC1 in regulating transcriptional gene repression.

In contrast to previous reports that put the direct repression of *Cdkn2a* as a central mechanism behind PRC1 biological functions, our data demonstrate that *Cdkn2a* repression is not involved in PRC1-dependent control of intestinal homeostasis; this is consistent with recent findings of our laboratory using other model systems (Piunti et al., 2014). This result is very important, since it also uncouples the inactivation of *Cdkn2a* or p53 that are frequently found in intestinal tumors from the essential role of PRC1 in sustaining stem cell proprieties in pathological conditions.

Besides the regulation of *Cdkn2a* expression, previous studies have provided a limited characterization of the genome-wide activity of PcG proteins in adult tissues and little mechanistic insight for dissecting the relevant molecular pathways directly controlled by PcG proteins. In mouse ESCs, PRC1-dependent H2Aubq maintains the transcriptional repression of developmental regulators, thereby preserving pluripotency and preventing spontaneous differentiation of ESCs (Stock et al., 2007). Our analysis now demonstrates that loss of PRC1-dependent transcriptional repression did not result in a premature differentiation of the stem cell pool but rather profoundly altered their transcriptional identity, leading to the expression of several genes—including a large number of TFs—that do not belong to the intestinal lineage. Combining these results with genome-wide location analysis, we have shown that the vast majority of these genes are directly controlled by PRC1 activity. More importantly, these results strongly suggest that the main function of PRC1 in the intestinal epithelium is to ensure that tissue identity is maintained.

The loss of PRC1 activity induced a massive transcriptional upregulation of DNA-binding TFs. Intriguingly, several of these factors were previously connected to β-catenin activity acting as negative regulators of its transcriptional functions (Fujimi et al., 2012; Ito et al., 2008; Jung et al., 2004, 2005; Pourebrahim et al., 2011; Sinner et al., 2007). Wnt-dependent transcription is crucially important for ISC maintenance, and its negative regulators can strongly affect the stem cell niche, leading to loss of the intestinal architecture and morbidity (Clevers et al., 2014). Focusing our attention on the family of Zic TFs, which were previously shown to inhibit β-catenin–induced axis duplication in *Xenopus* embryos (Fujimi et al., 2012; Pourebrahim et al., 2011), we observed that Zic proteins bind efficiently to the β-catenin/Tcf7l2 transcription complex, and that the activation of Zics expression inhibits the transcriptional activity of a constitutively activated form of β-catenin and impaired crypt homeostasis in 3D organoids cultures.

Figure 7. PRC1 Activity Is Essential for Wnt-Dependent Transcriptional Activity and Oncogenic Potential

(A) Tcf7l2 occupancy at defined loci in WT and PRC1 null ISCs or crypts.

(B) Venn diagram representing the overlap of Tcf7l2 peaks identified by ChIP-seq analysis performed with ISCs purified from WT or *Ring1a*$^{-/-}$ *Ring1b*$^{-/-}$ *Lgr5*$^{GFP\text{-}CreERT2}$ mice 6 days after tamoxifen injection.

(C) Cumulative Tcf7l2 ChIP-seq signal in WT or *Ring1a*$^{-/-}$ *Ring1b*$^{-/-}$ ISCs, purified from *Lgr5*$^{GFP\text{-}CreERT2}$ mice 6 days after tamoxifen treatment, at ±5 kb around the summit of Tcf7l2 peaks detected in WT crypts.

(D) Heatmap representing the normalized Tcf7l2 ChIP-seq intensities ±5 kb around the summit of all peaks identified in WT and PRC1-deficient ISCs 6 days after tamoxifen injection.

(E) Histological and immunohistochemical analyses of intestinal samples from mice expressing ISC-specific oncogenic β-catenin in the presence or absence of PRC1. H&E and Ki67 staining were performed 30 days after tamoxifen injection.

(F) Whole intestinal quantification of GFP fluorescence emitted from counterselected tumors treated with corn oil (Oil) or tamoxifen (TAM).

(G) Purification and in vitro spheroid formation of escaping *Lgr5*$^{GFP\text{-}CreERT2}$ *Ring1a*$^{-/-}$ *Ring1b*$^{-/-}$ *Ctnnb1*$^{ex3/ex3}$. Spheroids were isolated and grown for 1 week always in the absence of both RSPO1 and Wnt3a and then treated with 4-OHT or vehicle (EtOH) as indicated in the figure.

Related to Figures S6 and S7.

In summary, our data provide strong evidence that PRC1 activity regulates the self-renewal and proliferation of ISCs by sustaining the transcriptional activity of Wnt/β-catenin signaling via repression of inhibitory factors under normal and pathological conditions. Since Wnt/β-catenin activity has relevant developmental functions also in other tissues (Clevers, 2006; Clevers et al., 2014), understanding to which extent the PRC1-mediated control of β-catenin transcriptional activity is relevant in other stem cell types remains an important matter of investigation for the future. In addition, because this regulatory mechanism acts downstream of the constitutive activation of β-catenin and bypasses the frequent inactivation of *Cdkn2a* found in intestinal tumors, our findings not only strengthen the fundamental characterization of epigenetic mechanisms that control intestinal homeostasis, but also provide important knowledge that could stimulate development of potential therapeutic interventions for cancer treatment.

EXPERIMENTAL PROCEDURES

Animal Procedures

Mice were housed accordingly to the guidelines set out in Commission Recommendation 2007/526/EC, June 18, 2007, on guidelines for the accommodation and care of animals used for experimental and other scientific purposes. All experiments were performed in accordance with the Italian Laws (D.L.vo 116/92 and following additions), which enforces EU 86/609 Directive (Council Directive 86/609/EEC of 24 November 1986 on the approximation of laws, regulations, and administrative provisions of the Member States regarding the protection of animals used for experimental and other scientific purposes).

Minigut Culture

Minigut culture was performed according to (Sato et al., 2009). Briefly, isolated small intestine was flushed with ice-cold PBS and opened longitudinally. Villi were scraped using glass coverslips, and the tissue was cut into small pieces. After incubation in 2 mM EDTA, the crypts were released by mechanical disaggregation. Purified crypts were embedded in Matrigel (BD Biosciences) and either directly used for minigut formation or trypsin-digested and used for FACS analysis or FACS sorting. Miniguts were cultured in Advanced DMEM/F12, supplemented with HEPES, GlutaMax, antibiotics, N2, retinoic acid–free B27 supplements, EGF (all from GE Healthcare), Noggin (Preprotech), and mRSPO1 (R&D System). For ISC cultures, recombinant Wnt3a (Cell Guidance System), Jagged1 peptide (AnaSpec), and 10 μM Y-27632 (Selleck Chemicals) were also used. Growth factors were added daily, and the medium was replaced every 4 days. Cre-dependent recombination was induced using 4-hydroxytamoxifen (Sigma). For overexpression experiments, primary crypts or disaggregated organoids were transduced using lentiviral vectors as previously described (Koo et al., 2012). CMV-driven plasmid expressing ZIC1 or ZIC2 downstream to a lox-RFP-lox site or EF1α promoter-driven mutant (S33A; S37A; T41A; S45A) β-catenin were used to obtain protein expression. Transduced organoids were identified, respectively, for RFP positivity or selected for the ability to growth in selective medium without RSPO1 or Wnt3a.

Luciferase Assay

To evaluate TFC4-dependent transcriptional activity, luciferase assays were performed using TOP-Flash/FOP-flash assay as previously described (Korinek et al., 1997). A detailed description is available in the Supplemental Experimental Procedures.

Real-Time qPCR and Primers

Real-time qPCR was carried out using ABI7500 PCR machine (Applied Biosystem), and a reaction mix was prepared using Go Taq qPCR master mix (Promega) following manufacturer instructions. Primers sequences are available upon request.

ChIP-Seq and RNA-Seq Procedure, Sample Preparation, and Post-Sequencing Analysis

A detailed description of the procedures used for preparing RNA and DNA samples for sequencing together with post-sequencing analysis and annotations is available in the Supplemental Experimental Procedures.

ACCESSION NUMBERS

The accession number for the ChIP-seq and RNA-seq data reported in this paper is GEO: GSE65322.

SUPPLEMENTAL INFORMATION

Supplemental Information includes Supplemental Experimental Procedures, seven figures, and seven tables and can be found with this article online at http://dx.doi.org/10.1016/j.stem.2015.09.019.

AUTHOR CONTRIBUTIONS

F.C. and A.R. performed all the experimental work. S.J. performed the bioinformatics analysis. A.P. generated all $R26^{CreERT2}$ $Cdkn2a^{-/-}$ mouse strains. A.S. generated the Ring1b antibody. P.O.M. and J.H. provided the lox-RFP-lox inducible vector, and H.K. provided the *Ring1a* KO and *Ring1b* cKO mice. F.C., A.R., S.J., and D.P. analyzed the data. F.C., A.R., and D.P. conceived the experiments and wrote the manuscript.

ACKNOWLEDGMENTS

We thank Veronica Raker for editing support, Makoto Taketo for the $Ctnnb1^{ex3}$ mice, Miguel Vidal for the *Ring1a* and *Ring1b* KO mice, Elisabetta Dejana for support with mice, and Didier Negre for the inducible lentiviral backbone. We thank all members of the D.P. group for helpful discussions. The work in the D.P. laboratory was supported by grants from the Italian Association for Cancer Research (AIRC), the Italian Ministry of Health, and the Umberto Veronesi Foundation (FUV). A.R., A.P., and A.S. were supported by fellowships from the Italian Foundation for Cancer Research (FIRC). F.C. was supported by an FUV fellowship.

Received: March 6, 2015
Revised: August 11, 2015
Accepted: September 15, 2015
Published: October 29, 2015

REFERENCES

Aloia, L., Di Stefano, B., and Di Croce, L. (2013). Polycomb complexes in stem cells and embryonic development. Development *140*, 2525–2534.

Barker, N. (2014). Adult intestinal stem cells: critical drivers of epithelial homeostasis and regeneration. Nat. Rev. Mol. Cell Biol. *15*, 19–33.

Barker, N., van Es, J.H., Kuipers, J., Kujala, P., van den Born, M., Cozijnsen, M., Haegebarth, A., Korving, J., Begthel, H., Peters, P.J., and Clevers, H. (2007). Identification of stem cells in small intestine and colon by marker gene Lgr5. Nature *449*, 1003–1007.

Barker, N., Bartfeld, S., and Clevers, H. (2010). Tissue-resident adult stem cell populations of rapidly self-renewing organs. Cell Stem Cell *7*, 656–670.

Blackledge, N.P., Farcas, A.M., Kondo, T., King, H.W., McGouran, J.F., Hanssen, L.L., Ito, S., Cooper, S., Kondo, K., Koseki, Y., et al. (2014). Variant PRC1 complex-dependent H2A ubiquitylation drives PRC2 recruitment and polycomb domain formation. Cell *157*, 1445–1459.

Clevers, H. (2006). Wnt/beta-catenin signaling in development and disease. Cell *127*, 469–480.

Clevers, H., Loh, K.M., and Nusse, R. (2014). Stem cell signaling. An integral program for tissue renewal and regeneration: Wnt signaling and stem cell control. Science *346*, 1248012.

Cooper, S., Dienstbier, M., Hassan, R., Schermelleh, L., Sharif, J., Blackledge, N.P., De Marco, V., Elderkin, S., Koseki, H., Klose, R., et al. (2014). Targeting

polycomb to pericentric heterochromatin in embryonic stem cells reveals a role for H2AK119u1 in PRC2 recruitment. Cell Rep. *7*, 1456–1470.

de Napoles, M., Mermoud, J.E., Wakao, R., Tang, Y.A., Endoh, M., Appanah, R., Nesterova, T.B., Silva, J., Otte, A.P., Vidal, M., et al. (2004). Polycomb group proteins Ring1A/B link ubiquitylation of histone H2A to heritable gene silencing and X inactivation. Dev. Cell *7*, 663–676.

del Mar Lorente, M., Marcos-Gutiérrez, C., Pérez, C., Schoorlemmer, J., Ramírez, A., Magin, T., and Vidal, M. (2000). Loss- and gain-of-function mutations show a polycomb group function for Ring1A in mice. Development *127*, 5093–5100.

Endoh, M., Endo, T.A., Endoh, T., Isono, K., Sharif, J., Ohara, O., Toyoda, T., Ito, T., Eskeland, R., Bickmore, W.A., et al. (2012). Histone H2A mono-ubiquitination is a crucial step to mediate PRC1-dependent repression of developmental genes to maintain ES cell identity. PLoS Genet. *8*, e1002774.

Fevr, T., Robine, S., Louvard, D., and Huelsken, J. (2007). Wnt/beta-catenin is essential for intestinal homeostasis and maintenance of intestinal stem cells. Mol. Cell. Biol. *27*, 7551–7559.

Fujimi, T.J., Hatayama, M., and Aruga, J. (2012). Xenopus Zic3 controls notochord and organizer development through suppression of the Wnt/β-catenin signaling pathway. Dev. Biol. *361*, 220–231.

Gao, Z., Zhang, J., Bonasio, R., Strino, F., Sawai, A., Parisi, F., Kluger, Y., and Reinberg, D. (2012). PCGF homologs, CBX proteins, and RYBP define functionally distinct PRC1 family complexes. Mol. Cell *45*, 344–356.

Harada, N., Tamai, Y., Ishikawa, T., Sauer, B., Takaku, K., Oshima, M., and Taketo, M.M. (1999). Intestinal polyposis in mice with a dominant stable mutation of the beta-catenin gene. EMBO J. *18*, 5931–5942.

Ito, K., Lim, A.C., Salto-Tellez, M., Motoda, L., Osato, M., Chuang, L.S., Lee, C.W., Voon, D.C., Koo, J.K., Wang, H., et al. (2008). RUNX3 attenuates beta-catenin/T cell factors in intestinal tumorigenesis. Cancer Cell *14*, 226–237.

Johnson, V., Volikos, E., Halford, S.E., Eftekhar Sadat, E.T., Popat, S., Talbot, I., Truninger, K., Martin, J., Jass, J., Houlston, R., et al. (2005). Exon 3 beta-catenin mutations are specifically associated with colorectal carcinomas in hereditary non-polyposis colorectal cancer syndrome. Gut *54*, 264–267.

Jung, C., Kim, R.S., Lee, S.J., Wang, C., and Jeng, M.H. (2004). HOXB13 homeodomain protein suppresses the growth of prostate cancer cells by the negative regulation of T-cell factor 4. Cancer Res. *64*, 3046–3051.

Jung, C., Kim, R.S., Zhang, H., Lee, S.J., Sheng, H., Loehrer, P.J., Gardner, T.A., Jeng, M.H., and Kao, C. (2005). HOXB13 is downregulated in colorectal cancer to confer TCF4-mediated transactivation. Br. J. Cancer *92*, 2233–2239.

Kalb, R., Latwiel, S., Baymaz, H.I., Jansen, P.W., Müller, C.W., Vermeulen, M., and Müller, J. (2014). Histone H2A monoubiquitination promotes histone H3 methylation in Polycomb repression. Nat. Struct. Mol. Biol. *21*, 569–571.

Koo, B.K., Stange, D.E., Sato, T., Karthaus, W., Farin, H.F., Huch, M., van Es, J.H., and Clevers, H. (2012). Controlled gene expression in primary Lgr5 organoid cultures. Nat. Methods *9*, 81–83.

Korinek, V., Barker, N., Morin, P.J., van Wichen, D., de Weger, R., Kinzler, K.W., Vogelstein, B., and Clevers, H. (1997). Constitutive transcriptional activation by a beta-catenin-Tcf complex in APC-/- colon carcinoma. Science *275*, 1784–1787.

Korinek, V., Barker, N., Moerer, P., van Donselaar, E., Huls, G., Peters, P.J., and Clevers, H. (1998). Depletion of epithelial stem-cell compartments in the small intestine of mice lacking Tcf-4. Nat. Genet. *19*, 379–383.

Morin, P.J., Sparks, A.B., Korinek, V., Barker, N., Clevers, H., Vogelstein, B., and Kinzler, K.W. (1997). Activation of beta-catenin-Tcf signaling in colon cancer by mutations in beta-catenin or APC. Science *275*, 1787–1790.

Piunti, A., Rossi, A., Cerutti, A., Albert, M., Jammula, S., Scelfo, A., Cedrone, L., Fragola, G., Olsson, L., Koseki, H., et al. (2014). Polycomb proteins control proliferation and transformation independently of cell cycle checkpoints by regulating DNA replication. Nat. Commun. *5*, 3649.

Popov, N., and Gil, J. (2010). Epigenetic regulation of the INK4b-ARF-INK4a locus: in sickness and in health. Epigenetics *5*, 685–690.

Posfai, E., Kunzmann, R., Brochard, V., Salvaing, J., Cabuy, E., Roloff, T.C., Liu, Z., Tardat, M., van Lohuizen, M., Vidal, M., et al. (2012). Polycomb function during oogenesis is required for mouse embryonic development. Genes Dev. *26*, 920–932.

Pourebrahim, R., Houtmeyers, R., Ghogomu, S., Janssens, S., Thelie, A., Tran, H.T., Langenberg, T., Vleminckx, K., Bellefroid, E., Cassiman, J.J., and Tejpar, S. (2011). Transcription factor Zic2 inhibits Wnt/β-catenin protein signaling. J. Biol. Chem. *286*, 37732–37740.

Sato, T., Vries, R.G., Snippert, H.J., van de Wetering, M., Barker, N., Stange, D.E., van Es, J.H., Abo, A., Kujala, P., Peters, P.J., and Clevers, H. (2009). Single Lgr5 stem cells build crypt-villus structures in vitro without a mesenchymal niche. Nature *459*, 262–265.

Sato, T., van Es, J.H., Snippert, H.J., Stange, D.E., Vries, R.G., van den Born, M., Barker, N., Shroyer, N.F., van de Wetering, M., and Clevers, H. (2011). Paneth cells constitute the niche for Lgr5 stem cells in intestinal crypts. Nature *469*, 415–418.

Scelfo, A., Piunti, A., and Pasini, D. (2014). The controversial role of the Polycomb group proteins in transcription and cancer: how much do we not understand Polycomb proteins? FEBS J. *282*, 1703–1722.

Serrano, M., Lee, H., Chin, L., Cordon-Cardo, C., Beach, D., and DePinho, R.A. (1996). Role of the INK4a locus in tumor suppression and cell mortality. Cell *85*, 27–37.

Sinner, D., Kordich, J.J., Spence, J.R., Opoka, R., Rankin, S., Lin, S.C., Jonatan, D., Zorn, A.M., and Wells, J.M. (2007). Sox17 and Sox4 differentially regulate beta-catenin/T-cell factor activity and proliferation of colon carcinoma cells. Mol. Cell. Biol. *27*, 7802–7815.

Snippert, H.J., van der Flier, L.G., Sato, T., van Es, J.H., van den Born, M., Kroon-Veenboer, C., Barker, N., Klein, A.M., van Rheenen, J., Simons, B.D., and Clevers, H. (2010). Intestinal crypt homeostasis results from neutral competition between symmetrically dividing Lgr5 stem cells. Cell *143*, 134–144.

Soriano, P. (1999). Generalized lacZ expression with the ROSA26 Cre reporter strain. Nat. Genet. *21*, 70–71.

Stock, J.K., Giadrossi, S., Casanova, M., Brookes, E., Vidal, M., Koseki, H., Brockdorff, N., Fisher, A.G., and Pombo, A. (2007). Ring1-mediated ubiquitination of H2A restrains poised RNA polymerase II at bivalent genes in mouse ES cells. Nat. Cell Biol. *9*, 1428–1435.

van der Flier, L.G., and Clevers, H. (2009). Stem cells, self-renewal, and differentiation in the intestinal epithelium. Annu. Rev. Physiol. *71*, 241–260.

van Es, J.H., Haegebarth, A., Kujala, P., Itzkovitz, S., Koo, B.K., Boj, S.F., Korving, J., van den Born, M., van Oudenaarden, A., Robine, S., and Clevers, H. (2012). A critical role for the Wnt effector Tcf4 in adult intestinal homeostatic self-renewal. Mol. Cell. Biol. *32*, 1918–1927.

Voncken, J.W., Roelen, B.A., Roefs, M., de Vries, S., Verhoeven, E., Marino, S., Deschamps, J., and van Lohuizen, M. (2003). Rnf2 (Ring1b) deficiency causes gastrulation arrest and cell cycle inhibition. Proc. Natl. Acad. Sci. USA *100*, 2468–2473.